

# A Model of Proton Pumps in an Electric Field: the Impact of Grotthuss Mechanism on Charge Translocation

Natalie Pavlenko[\*] and Thor Stasyuk

Institute for Condensed Matter Physics,  
1 Svientsitsky St., UA-79011, Lviv, Ukraine

(Dated: January 7, 2019)

## Abstract

We present the results of the modeling of proton translocation in finite H-bonded chains in the framework of two-stage proton transport model. We explore the influence of reorientation motion of protons, as well as the effect of electric field and proton correlations on system dynamics. An increase of the reorientation energy results in the transition of proton charge from the surrounding to the inner water molecules in the chain. Proton migration along the chain in an external electric field has a step-like character, proceeding with the occurrence of electric field threshold-type effects and drastic redistribution of proton charge. Electric field applied to correlated chains induces first a formation of ordered dipole structures for lower field strength, and then, with a further field strength increase, a stabilization of states with Bjerrum D-defects.

PACS numbers: 87.16.Xx, 72.20.Ek, 86.16.Jv

## I. INTRODUCTION

Translocation of protons over long distances has a key importance for biological systems. It is believed that proton migration along the chains of water molecules formed between the interior of proteins and the solvent, establishes electrochemical potential gradients playing an important functional role [1]. Experimental evidence indicates that the dominant mechanism responsible for proton transport in transmembrane proteins (for instance, in bacteriorhodopsin of *Halobacterium halobium* [2, 3] and in gramicidin A channels [3, 4]) is the diffusion of  $H^+$  ions which is faster than the hydrodynamic flow of hydronium species  $(H_3O)^+$ . Especially at low hydrogen concentrations in channels, proton conduction is determined by a two-stage Grotthuss-type mechanism [5, 6] shown schematically in Fig. 1 (a). The first stage involves the intrabond proton tunnelling along the hydrogen bridge which is connected with the transfer of ionic positive and negative charged defects. To sustain a flux of  $H^+$  in such proton wire, the intermolecular proton transfer due to the reorientations of molecular group with proton is assumed. Reorientation motion leads to the breaking of the hydrogen bond (so-called orientational Bjerrum L-defect) and location of proton between another pair of molecular groups. Consequently, reorientation step in the presence of the second proton may induce high-energy configuration with both of the protons shared by two adjacent oxygen ions (Bjerrum D-defect). Thus the second stage of transport process involving a migration of Bjerrum defects is the rate-limiting step for the rapid proton migration [7].

As was pointed in [5], experimental analysis of proton flow in bioenergetic proteins and mechanism of proton migration is very difficult because of its intrinsically transient nature. To shed more light on microscopic nature of proton transport and to analyze influence of quantum effects and interaction with proton surrounding, theoretical modeling remains to be essentially important.

The goal of the present work is to study proton wire containing a finite number of water molecules by the use of quantum statistical mechanics methods which are extremely effective in the description of collective nature of proton transfer and in quantum treatment of light H nuclei [8]. To describe correctly proton transport process, we employ here two-stage proton transport model [9] incorporating quantum effects such as proton tunneling and zero-point vibration energy. In earlier papers [10, 11, 12] we applied two-stage model to analyze effect of

coupling between protons and molecular group vibrations on proton conductivity in infinite H-bonded chains. In particular, it was shown that the proton-lattice vibration interactions induce structural instabilities and charge ordering in system [10], whereas the Grotthus-type transport mechanism manifests itself in nontrivial temperature- and frequency dependences of proton conductivity [11, 12].

In this work, in order to study proton migration in finite biological systems, we analyze the influence of proton-proton correlations, comparing two different protonated chains containing one and two excess protons respectively. We find that the reaction of protonation of water chain is extremely sensitive to the reorientation energy of proton motion. We show that the increase of reorientation energy results in the drastic decrease of the proton charge density at the boundary between the chain and surrounding with consequent localization of protons near the inner water molecules. Moreover, as appeared from our modeling, the application of external electric field induces the step-like threshold-type effects with the ordering of proton charge and stabilization of Bjerrum D-defects in the wire.

## II. MODEL SPECIFICATION AND METHOD OF CALCULATION

To model a proton wire, we consider a linear chain containing  $N$  hydrogen bonds and  $l = 1; 2; \dots; N; N + 1$  molecular groups. The outer left ( $l = 1$ ) and right ( $l = N + 1$ ) molecular complexes mimic the surrounding of the proton wire and differ from the inner ( $l = 2; \dots; N$ ) water molecules. The transport of excess proton through the wire proceeds via the following two steps:

(i) proton can be transferred within a H-bond (process shown by short arrows in Fig. 1 (a)) which is modelled by simple two-minimum potential, with corresponding tunneling integral

$T$ :

$$H_T = \sum_{l=1}^{N+1} (c_{la}^\dagger c_{lb} + c_{lb}^\dagger c_{la}); \quad (1)$$

where  $c_l^\dagger$  ( $c_l$ ) are the operators of the proton creation (annihilation) in the position  $(l, \alpha)$  (the index  $\alpha = fa; bg$  denotes left/right position for proton on the H-bond);

(ii) a water molecule together with covalently bonded hydrogen ion can be rotated, and this process causes the breaking of the H-bond and location of  $H^+$  between two another nearest

water molecules of the wire (process depicted by long arrows in Fig. 1 (a)):

$$H_R = \sum_{l=1}^N R_l (c_{l+1,a}^\dagger c_{l,b} + c_{l,b}^\dagger c_{l+1,a}); \quad (2)$$

where  $R_l$  is reorientation energy for proton introduced here in analogy with the intra-bond transfer term (1).

Besides the transport process, we incorporate the following two types of interactions between protons in the chain:

(iii) different short-range configurations of the protons near an inner water molecule as well as an outer molecular group can appear due to the different nature of bonding (shorter covalent or longer H-bond). The energies of possible configurations (shown in Fig. 1 (b)) are described by the following terms:

$$\begin{aligned} H_1 &= u_1 (1 - n_{1a}) + w_1 n_{1a}; \quad H_{N+1} = u_{N+1} (1 - n_{Nb}) + w_{N+1} n_{Nb}; \\ H_l &= w^0 (1 - n_{l+1,a}) (1 - n_{l,b}) + w n_{l+1,a} n_{l,b} + u (1 - n_{l,b}) n_{l+1,a} + u n_{l,b} (1 - n_{l+1,a}); \end{aligned} \quad (3)$$

The parts  $H_1$  and  $H_{N+1}$  describe the energies of the boundary proton configurations near the left and the right surrounding molecular groups (we assume for simplicity  $u_1 = u_{N+1} = u$  and  $w_1 = w_{N+1} = w$  in the boundary configurations shown in the upper scheme of Fig. 1 (b)). The terms  $H_l$  ( $l = 2; \dots; N$ ) contain the configuration energies for the water molecules in the wire (the lower part in Fig. 1 (b)). Here the proton occupancy operators  $n_l = c_l^\dagger c_l = f_{0;1g}$ ; (IV) a strong repulsion between two nearest protons shared by two neighboring oxygens (so called Bjerrum D-defect) with repulsion energy  $U$  is represented by the term:

$$H_C = U \sum_{l=1}^N n_{la} n_{lb}; \quad (4)$$

In our following analysis we use the value of  $U = 10$  kcal/mol corresponding to the energy of relaxed D-defect estimated in [13] on the basis of quantum chemical calculations.

To model a field exerted by the surrounding, we apply an external electric field of the strength  $E$  to the proton wire, which is described by the following term

$$e_p E \sum_{l=1}^N R_l n_l; \quad (5)$$

where  $R_l$  is the coordinate of the proton position ( $l$ , ) with respect to the center of the chain, and  $e_p$  denotes the proton charge.

In order to analyze the dynamics of the proton wire embedded in the surrounding under the influence of the field, as well as the effect of rotational motions of covalent groups with proton, we will focus our attention on the polarization of the proton wire given by

$$P = e_p \langle \sum_{l=1}^N R_l n_l \rangle; \quad (6)$$

$= \langle f_a, b_g \rangle$

where  $\langle \dots \rangle$  denotes statistical average with respect to the system energy (1-5). The average probabilities  $n_l$  of occupation of the position  $(l)$  by proton describe the distribution of the proton charge in the wire, and thus is another very important characteristics to track the proton migration.

To calculate exactly the above-mentioned statistical averages, we need to know the quantum energy levels determined by the energy (1-5). This can be done by a mapping of the proton states  $(l)$  on the multi-site basis  $|j\rangle = |j_{1a}; j_{1b}; \dots; j_{Nb}\rangle$ . Then, using the projection operators  $X^{ii^0} = |j\rangle\langle i|$  acting on the new basis  $|j\rangle$  we rewrite the system energy (1-5) in convenient form:

$$H = H^0 + H^1 + \dots + H^{2N}; \quad (7)$$

Each term  $H^{n_p}$  in (7) corresponds exactly to  $n_p$  protons in the chain ( $n_p = 0, 1, \dots, 2N$ ). This means in fact that the mapping on the states  $|j\rangle$  allows to decompose the terms (1-5) and analyze the cases of different number of protons in the wire separately.

We demonstrate below the procedure of the mapping in the system with  $N = 2$  H-bonds on the multi-site states. For  $N = 2$  the basis  $|j\rangle$  includes  $2^{2N} = 16$  states  $|j_{1a}; j_{1b}; j_{2a}; j_{2b}\rangle$ :

$$\begin{aligned} |1\rangle &= |0000\rangle; |2\rangle = |1000\rangle; |3\rangle = |0100\rangle; \\ |4\rangle &= |0010\rangle; |5\rangle = |0001\rangle; |6\rangle = |1100\rangle; \\ |7\rangle &= |1010\rangle; |8\rangle = |1001\rangle; |9\rangle = |0110\rangle; \\ |10\rangle &= |0101\rangle; |11\rangle = |0011\rangle; \dots; |16\rangle = |1111\rangle; \end{aligned} \quad (8)$$

We can derive the relations between  $c_{ij}$  and  $X^{ii^0} = |j\rangle\langle i|$ :

$$c_{ij} = \sum_{i,j} X^{ij} c_i; \quad |j\rangle X^{ij}; \quad (9)$$

where the expectation numbers  $\langle X^{ij} \rangle$ ,  $|j\rangle$  can be found using the usual antisymmetric rules

for Fermi operators [14]. Specifically, for the case  $N = 2$  the expressions (9) yield:

$$\begin{aligned}
C_{0;a} &= X^{1;2} + X^{3;6} + X^{4;7} + X^{5;8} + X^{9;12} + X^{10;13} + X^{11;14} + X^{15;16} \\
C_{1;a} &= X^{1;4} - X^{2;7} - X^{3;9} + X^{5;11} + X^{6;12} - X^{8;14} - X^{10;15} + X^{13;16} \\
C_{0;b} &= X^{1;3} - X^{2;6} + X^{4;9} + X^{5;10} - X^{7;12} - X^{8;13} + X^{11;15} - X^{14;16} \\
C_{1;b} &= X^{1;5} - X^{2;8} - X^{3;10} - X^{4;11} + X^{6;13} + X^{7;14} + X^{9;15} - X^{12;16}
\end{aligned} \tag{10}$$

Using the relations (10) and the fact that  $X^{ii^0} X^{1l^0} = \delta_{i^0 l^0} X^{ii^0}$  (due to the orthogonality of the states  $j|i$ ), we decompose (1-5) in terms of  $X^{ii^0}$  operators into the following 5 terms:

$$H = H_2^0 + H_2^1 + H_2^2 + H_2^3 + H_2^4; \tag{11}$$

where

$$\begin{aligned}
H_2^0 &= a_2^0; \\
H_2^1 &= (U + (J_r + J_{ab})E)X^{2;2} + J_r E (X^{3;3} - X^{4;4}) + \\
&\quad (U - (J_r + J_{ab})E)X^{5;5} + J_T (X^{2;3} + X^{3;2}) + \\
&\quad J_T (X^{4;5} + X^{5;4}) + J_R (X^{3;4} + X^{4;3}) + a_2^1;
\end{aligned} \tag{12}$$

$$\begin{aligned}
H_2^2 &= (U + (2J_r + J_{ab})E)X^{6;6} + J_{ab} (X^{7;7} - X^{10;10}) + \\
&\quad X^{8;8} + (J_T - J_R)X^{9;9} + (U - (2J_r + J_{ab})E)X^{11;11} + \\
&\quad J_T (X^{7;8} + X^{8;7}) + J_T (X^{8;10} + X^{10;8}) + J_T (X^{9;10} + X^{10;9}) + \\
&\quad J_R (X^{6;7} + X^{7;6}) + J_R (X^{10;11} + X^{11;10}) + a_2^2;
\end{aligned} \tag{13}$$

$$\begin{aligned}
H_2^3 &= (U + J_T + (J_r + J_{ab})E)X^{12;12} + (U + J_r E)X^{13;13} + \\
&\quad (U - J_r E)X^{14;14} + (U + J_T - (J_r + J_{ab})E)X^{15;15} + \\
&\quad J_T (X^{12;13} + X^{13;12}) + J_T (X^{14;15} + X^{15;14}) + \\
&\quad J_R (X^{13;14} + X^{14;13}) + a_2^3;
\end{aligned} \tag{14}$$

$$H_2^4 = (2U + J)X^{16;16} + a_2^4;$$

Since the parameter  $\epsilon_l = (w_l - w^0) / (w^0)$  in (12)-(14) is the difference between proton configuration energies at the boundary ( $l = 1$  or  $l = N + 1$  surrounding molecular groups), and at the inner ( $2 < l < N$ ) water molecule, it describes, in fact, the energy barrier for

the protonation of the water chain. For our analysis  $\epsilon$  has the key importance, because the other energy constants in (12)–(14)

$$\begin{aligned} a_2^0 &= a_2^2 - (w + u) - (w^0); & a_2^1 &= a_2^2 - (w + u); \\ a_2^3 &= a_2^2 + (w + u); & a_2^4 &= a_2^2 + (w + u) + (w^0); \\ a_2^5 &= w + u + w^0 \end{aligned}$$

which appear due to the boundary effects, are independent of the proton location in the wire and thus do not influence the statistical characteristics like (6). Analogously to [9], we consider below the case  $\epsilon < 0$  (taking  $j = 0.85$  kcal/mol in our numerical calculations), when the proton is attracted to the surrounding and needs to overcome the boundary energy barrier  $j$  to protonate the water chain.

The parameter  $J = w + w^0 - 2u$  describes the effective short-range interaction between protons near the water molecule. Because  $J$  includes the two-proton configuration energy  $w$  (see Fig. 1 (b)) and the value of  $w$  is one-two orders of magnitude higher than the values of  $u$  and  $w^0$  (the later is in agreement with the results obtained in [15]), we set in the following analysis  $J \gg 1$  excluding in this way the appearance of these two-proton configurations in our system.

Due to the two types of motions we have two different contributions to the proton dipole moment: the orientational part  $\mu_r = e_p R_r$  and the transfer part  $\mu_{ab} = e_p R_{ab}$  where  $R_{ab} = R_{jb} - R_{ja}$  denotes the distance H–H between two nearest proton positions of the H-bond. In our calculations, we use the values  $\mu_{ab} = 3.5$  D and  $\mu_r = 4.5$  D corresponding to the moderately strong H-bond with O–O distance  $R_{ab} + 2R_r = 2.6$  Å and the covalent O–H bond with the length  $R_r = 0.94$  Å.

By the similar way the energy (1–5) can be rewritten for the system with any finite value of  $N$ .

### III. CASE STUDY: ONE EXCESS PROTON IN CHAIN

As the starting point, in this section we mimic the situation when one proton is moved towards the water chain embedded into the solvent. To examine the behavior of the protonated chain with  $N$  H-bonds and  $n = 1$  excess proton, we consider  $H^{-1}$  part of the energy given by (11). Since the zero-point vibration energy for protonated chains is larger than

the potential energy barrier for the proton transfer between two shared oxygens [17], the quantum tunneling is not required for intra-bond  $H^+$  transfer. Thus, in our modelling we set  $T = 0$ . With this assumption, the energy levels of  $H^+$  can be found exactly:

$$\begin{aligned} \epsilon_{1,2} &= (N-1)\epsilon_r + \frac{N}{2}\epsilon_{ab} \pm E; \\ \epsilon_{3;\dots;2N} &= \begin{cases} i(-\frac{\epsilon_{ab}}{2} + \epsilon_r)E \pm p & (i=1;3;\dots;N-2); \text{ for odd } N \\ i(-\frac{\epsilon_{ab}}{2} + \epsilon_r)E \pm p & (i=0;2;\dots;N-2); \text{ for even } N \end{cases} \end{aligned} \quad (15)$$

where  $p = \frac{p}{\sqrt{\epsilon_r^2 E^2 + \frac{1}{4}\epsilon_r^2}}$ .

To analyze the role of  $\epsilon_r$  we consider first the case without external field ( $E = 0$ ). Depending on the value of  $\epsilon_r$ , two different regimes may be stabilized in the system. In the first small- $\epsilon_r$  regime, the two lowest energy levels  $\epsilon_{1,2}$  correspond to the superposition of the two boundary states

$$|j0\dots00i\rangle \text{ and } |j0\dots01i\rangle \quad (16)$$

with the proton located in the surrounding near the left or the right outer molecular groups. In the second large- $\epsilon_r$  regime the proton is shared between the inner water molecules of the chain and the ground states of the system corresponds to the superposition of the states

$$|j10\dots00i\rangle; |j010\dots00i\rangle; \dots; |j0\dots010i\rangle \quad (17)$$

with the energies  $\epsilon_{3;\dots;2N}$ . The "critical" value  $\epsilon_r = \epsilon_{cr}$  separating these two regimes, reflects the transition of the proton from the surrounding to the states where the proton is shared by the chain water molecules, which corresponds to the protonation chemical reaction. Fig. 2 shows the variation of the average occupancies of proton sites with  $\epsilon_r$  for the chains with  $N = 2$  and  $N = 3$  H-bonds. At  $\epsilon_r = \epsilon_{cr}$  the boundary proton occupancies  $\langle n_{1a} \rangle = \langle n_{N-b} \rangle$  drop drastically to zero, whereas the occupation numbers of the central positions  $\langle n_{1b} \rangle = \dots = \langle n_{N-1} \rangle$  increase up to the value  $\frac{1}{2(N-1)}$ , reflecting the redistribution of collectivized proton between the inner sites in the wire. This fact is supported by the results reported in [16, 17] showing that in H-bonded finite chains, the excess charge is best solvated by the central H-bonds. Moreover, as follows from our results, to overcome the barrier between the surrounding and the wire, the reorientation energy should be sufficiently large ( $\epsilon_r > \epsilon_{cr}$ ) in order to stabilize the inner proton configurations.



We turn now to an analysis of the proton translocation directed by the external field (the case  $E \neq 0$ ). Fig. 3 shows the field-dependences of  $P$  and  $\ln I$  for the chain containing  $N = 2$  H-bonds. We note that the behavior in the first small- and in the second large- $R$  regime differs drastically. In the small- $R$  regime the polarization increases smoothly with  $E$  approaching finally its maximal saturation value  $P_{\max} = \epsilon_r + \epsilon_{ab}$  (Fig. 3(a), inset). In contrast to this, in the large- $R$  regime the field dependence is rather nontrivial: first for  $E < E_{\text{thresh}}$   $P$  changes very slowly, and then at  $E = E_{\text{thresh}}$  a strong increase of  $P$  to  $P = P_{\max}$  is observed in Fig. 3(a). This rapid step-like change of the proton polarization reflects the threshold-type effect with the threshold electric field value

$$E_{\text{thresh}} = \frac{\epsilon_H + \frac{P}{\epsilon_r + \epsilon_{ab}} \left( \frac{\epsilon_r^2}{\epsilon_H} + \frac{\epsilon_r^2}{\epsilon_{ab}} \right)}{\frac{\epsilon_r^2}{\epsilon_H} + \frac{\epsilon_r^2}{\epsilon_{ab}}}; \quad (\epsilon_H = \epsilon_r + \epsilon_{ab}) \quad (18)$$

which does not depend on the chain size  $N$  ( $E_{\text{thresh}} \approx 0.15 \cdot 10^7$  V/cm for the chains with  $N = 2$  as can be observed in Fig. 3(a)). As we see in Fig. 3(b), the proton charge translocation under the influence of field in this case proceeds not smoothly, but has a step-like character. As results from (18), the threshold value  $E_{\text{thresh}}$  (which is needed to overcome a barrier for pumping between the inner localized states (17) and the boundary state  $|0 \dots 0\rangle$  in the direction of field) increases for larger  $R$  (Fig. 3(a), the cases with  $R = 1.5$  kcal/mol and  $R = 2.15$  kcal/mol). Since the reorientation energy  $R$  depends on the number of water molecules in the chain [5], increasing for longer chains, the successive translocation of the excess proton in the wire under the influence of  $E$  should occur at the higher field values. This means, that the conductivity of protonated chains should drop with the increasing chain length, which is in agreement with the conclusion reported in [5].

#### IV. ROLE OF PROTON-PROTON CORRELATIONS

In order to examine the influence of proton correlations, we consider the translocation of two excess protons in the wire which is described by the part  $H^2$  of the total energy (11). Since the presence of two protons in wire may lead to the formation of Bjerrum D-defect, the energy  $H^2$  for the chain with  $N = 2$  H-bonds given by the expression (13), contains the terms with the energy  $U$  of the repulsion between two nearest-neighboring protons.

Analogously to the 1-proton wire, we analyze first the behavior of the chain without the electric field. For  $N = 2$  and  $T = 0$  the energy levels found from (13) have the following

form :

$$\begin{aligned}
\epsilon_{1,2} &= \frac{1}{2} (U - q) + \epsilon_H E; \\
\epsilon_3 &= \epsilon_4 = \epsilon_H + J; \\
\epsilon_{5,6} &= \frac{1}{2} (U - q_{\pm}) - \epsilon_H E; \quad (q = \frac{q}{(U - 2\epsilon_R E)^2 + 4\epsilon_R^2})
\end{aligned} \tag{19}$$

and correspond to the following states of the wire:

$$\begin{aligned}
|\psi_1\rangle &= \frac{p}{\epsilon_R^2 + p^2} |\phi_1\rangle + \frac{\epsilon_R}{\epsilon_R^2 + p^2} |\psi_1\rangle; \\
|\psi_2\rangle &= \frac{\epsilon_R}{\epsilon_R^2 + p^2} |\phi_1\rangle - \frac{p}{\epsilon_R^2 + p^2} |\psi_1\rangle; \\
|\psi_3\rangle &= |\psi_4\rangle; \quad |\psi_5\rangle = |\psi_6\rangle; \\
|\psi_5\rangle &= \frac{\epsilon_R}{\epsilon_R^2 + p_+^2} |\psi_{10}\rangle + \frac{p_+}{\epsilon_R^2 + p_+^2} |\psi_{11}\rangle; \\
|\psi_6\rangle &= -\frac{p_+}{\epsilon_R^2 + p_+^2} |\psi_{10}\rangle + \frac{\epsilon_R}{\epsilon_R^2 + p_+^2} |\psi_{11}\rangle
\end{aligned} \tag{20}$$

with  $p = \frac{1}{2} (U - q) - \epsilon_R E$ .

To study the influence of  $\epsilon_R$ , we analyze (19) and (20) for  $E = 0$  and put  $J = 1$  excluding in this way the high-energy configuration  $|\psi_1\rangle = |\psi_{110}\rangle$ . Similarly to the 1-proton wire, the two different regimes can exist in the system depending on the value of the reorientation energy. In the first small- $\epsilon_R$  regime (for  $\epsilon_R < \epsilon_R^{(2)} = \frac{p}{\epsilon_R^2 - U}$ ), each proton is located near the outer molecular group and the state  $|\psi_3\rangle = |\psi_{100}\rangle$  has the minimal energy  $\epsilon_3 = \epsilon_H$ . As  $\epsilon_R$  increases and approaches the "critical" value  $\epsilon_R^{(2)}$ , the transition to the large- $\epsilon_R$  regime occurs. In this regime (for  $\epsilon_R > \epsilon_R^{(2)}$ ) the lowest energy levels  $\epsilon_2 = \epsilon_6 = \frac{1}{2} (U - q)$  ( $q = q_{\pm}(E = 0) = q(E = 0)$ ) correspond to the states  $|\psi_2\rangle$  and  $|\psi_6\rangle$  in (20), with one proton located inside the wire. However, in contrast to the section III, the transition between these two regimes is  $U$ -dependent, because  $\epsilon_R^{(2)}$  contains the energy of the D-defect  $U$ . Fig. 4 shows the variation of the proton occupation numbers  $\ln_1$  with  $\epsilon_R$  for  $U = 9.4$  kcal/mol and  $U = 1.9$  kcal/mol (plotted in the inset). The "critical" value  $\epsilon_R^{(2)} = 3$  kcal/mol for the repulsion energy  $U = 9.4$  kcal/mol is larger as compared with  $\epsilon_R^{(2)} = 1.5$  kcal/mol for  $U = 1.9$  kcal/mol. So far as the repulsion energy  $U$  is significant,  $\epsilon_R^{(2)} > \epsilon_R$ . However, as  $U \rightarrow 0$ ,  $\epsilon_R^{(2)}$  approaches the "critical" value  $\epsilon_R$  for the one-proton case. Moreover, as we can see from (20) and (8), the ground states  $|\psi_2\rangle$  and  $|\psi_6\rangle$  in the large- $\epsilon_R$  regime are represented by the superpositions of the normal configurations  $|\psi_1\rangle$  and  $|\psi_{10}\rangle$  with the states

$|\beta\rangle$  and  $|\beta_{11}\rangle$  containing the D-defect. However, as  $U \rightarrow 1$ , the weight constants for the D-defect states in (20) become smaller:  $P_{\frac{R}{2} + \frac{1}{4} + p^2} = P_{\frac{R}{2} + \frac{1}{4} + (U-q)^2} \rightarrow 0$ . Thus, the contribution of the D-defect-states to the stable wire configuration goes down as  $\frac{1}{U}$  for the stronger proton repulsion  $U$  (see for the comparison  $\langle n_6 \rangle = \langle n_{11} \rangle$  for different  $U$  plotted in Fig. 4).

We study now the electric field effect in correlated chains. Fig. 5 shows the variation of polarization and redistribution of protons with increasing  $E$ . Consider first the small- $R$  regime. In distinct to the 1-proton wire, where the polarization increases smoothly to its maximal value  $P_{\max}$  (Fig. 3(a), inset), we observe here two different threshold effects. The first transition from the state  $|\beta\rangle$  of (8) (the ground state of the wire in the small- $R$  regime at  $E = 0$ ) to the state  $|\beta_{10}\rangle$  (where both of the protons are ordered in the right position of each H-bond in the direction of the field) occurs at the threshold field value

$$E_1 = \frac{(N-1)(2r + a_b) - 2r}{2r} : \quad (21)$$

The distribution of the occupation probabilities  $\langle n_8 \rangle$  and  $\langle n_{10} \rangle$  for the states  $|\beta\rangle$  and  $|\beta_{10}\rangle$  is plotted in Fig. 5(b). We observe at  $E = E_1$  the abrupt increase of  $\langle n_{10} \rangle$ , while at the same field value  $\langle n_8 \rangle$  drops to zero. Furthermore, we conclude from (21) that the value  $E_1$  lowers with the number  $N$  of the water molecules in the chain. This fact can be observed in Fig. 6 where the jumps of polarization are plotted for different  $N$ . Finally, for very long water chain ( $N \rightarrow 1$ )  $E_1 \rightarrow 0$ . In contrast to the strong  $N$ -dependence of  $E_1$ , the second threshold effect appears at

$$E_2 = \frac{U}{2r} \quad (22)$$

essentially due to the proton correlations and does not depend on the chain length. The strong increase of  $P$  at  $E = E_2$  shown in Fig. 5(a) and Fig. 6 is related to the second drastic redistribution of the proton charge in the wire. As can be observed in Fig. 5(b), at  $E = E_2$  the occupation probability  $\langle n_{11} \rangle$  of the D-defect-state  $|\beta_{11}\rangle$  drastically increases to 1, whereas  $\langle n_{10} \rangle$  drops to zero. Thus, as resulted from our model, the formation of D-defect in external electric field has a step-like character proceeding via the threshold mechanism. In the large- $R$  regime, where the protons are stabilized at the inner water molecules already at  $E = 0$ , the first threshold phenomenon at  $E = E_1$ , observed for the small- $R$  case, does not occur. However, the threshold transition at  $E = E_2$  with the formation of D-defect appears in this regime similarly to the regime of small  $R$ , that can be observed in  $P$ -profile for  $R = 3$  kcal/mol shown in Fig. 5(a).

## V . S U M M A R Y

In this work we studied the process of proton translocation in 1D-chains mimicking protonated water channels embedded in surrounding. We have analyzed the role of the reorientation motion of protons, as well as the effect of electric field and proton correlations on the chain dynamics. We have shown that the increase of the reorientation energy results in the transition to the large- $\epsilon_r$  regime characterized by the transfer of the proton charge from the surrounding to the inner water molecules in the chain. The process of proton migration along the chain in the external electric field has the step-like character leading to the appearance of the electric field threshold-type phenomena with drastic redistribution of proton charge. The correlations between protons in the chain increase the "critical" reorientation energy necessary for the transition into the large- $\epsilon_r$  regime. The electric field applied to correlated chains induces first the formation of ordered dipole structures for the lower  $E$  values, and then, with the further  $E$  increase, the stabilization of states with Bjerrum D-defects.

---

[\*] Present address: Institut für Theoretische Physik, Physik-Department der TU München,  
James-Frank-Strasse, D-85747 Garching b. München, Germany;

E-mail: natalie@physik.tu-muenchen.de

- [1] R.B. Gennis, Biomembranes: Molecular Structure and Functions (Springer-Verlag, 1989).
- [2] W. Stoeckenius, R.H. Lozier, and R.A. Bogomolni, Biochim. Biophys. Acta 505, 215 (1979).
- [3] J.F. Nagle and M. Mille, J. Chem. Phys. 74, 1367 (1981).
- [4] D.G. Levitt, S.R. Elias, and J.M. Hautman, Biochim. Biophys. Acta 512, 436 (1978).
- [5] S. Cukierman, Biophys. J. 78, 1825 (2000).
- [6] M.-S. Chen, L. Onsager, J. Bonner and J. Nagle, J. Chem. Phys. 60, 405 (1974).
- [7] J.F. Nagle, M. Mille, and H.J. Morowitz, J. Chem. Phys. 72, 3959 (1980).
- [8] A.S. Davydov, Biology and Quantum Mechanics (Pergamon Press, 1982).
- [9] I.V. Stasyuk, O.L. Ivankiv and N. Pavlenko, J. Phys. Stud. 1, 418 (1997).
- [10] N. Pavlenko, Phys. Rev. B 61, 4988 (2000).
- [11] N. Pavlenko, J. Chem. Phys. 112, 8637 (2000).
- [12] N. Pavlenko, Phys. Stat. Sol. (b) 218, 295 (2000).

- [13] R. Hassan, E. Campbell, J. Chem. Phys. 97, 4326 (1992).
- [14] A. S. Davydov, Quantum Mechanics (Pergamon Press, 1965).
- [15] M. Eckert, G. Zundel, J. Phys. Chem. 92, 7016 (1988).
- [16] R. Pomes, J. Phys. Chem. 100, 2519 (1996).
- [17] R. Pomes, Isr. J. Chem. 39, 387 (1999).

## Figure captions

Fig. 1. (a) Schematic presentation of proton wire, arrows indicate a possible path of proton migration along the chain. Full circles denote water molecules and open circles are the possible positions for excess proton. (b) Scheme of possible proton configurations near the outer surrounding groups (the upper part) and the inner water molecules of the wire (the lower part).

Fig. 2. Proton site occupancies for different reorientation energies  $\epsilon_R$  in the chain with two hydrogen bonds containing one excess proton. The inset shows the redistribution of proton charge in the chain with  $N = 3$  H-bonds.

Fig. 3. (a) Proton polarization vs electric field in the small- $\epsilon_R$  (shown in the inset)- and large- $\epsilon_R$  regimes for  $T = 30K$ , and (b) average site occupancies vs  $E$  in the chain containing  $N = 2$  hydrogen bonds and  $n = 1$  proton for  $\epsilon_R = 1.5$  kcal/mol and for different temperatures.

Fig. 4. Proton charge distribution vs  $\epsilon_R$  in the H-bonded chain ( $N = 2$ ) containing two protons ( $n = 2$ ) for  $T = 100K$ .

Fig. 5. (a) Proton polarization for different  $\epsilon_R$  and (b) average site occupancies for  $\epsilon_R = 0.43$  kcal/mol vs electric field  $E$  in the chain containing  $N = 2$  hydrogen bonds and  $n = 2$  protons;  $T = 30K$ .

Fig. 6. Proton polarization vs  $E$  in the chains of different length containing two protons for  $\epsilon_R = 0.43$  kcal/mol and  $T = 300K$ .

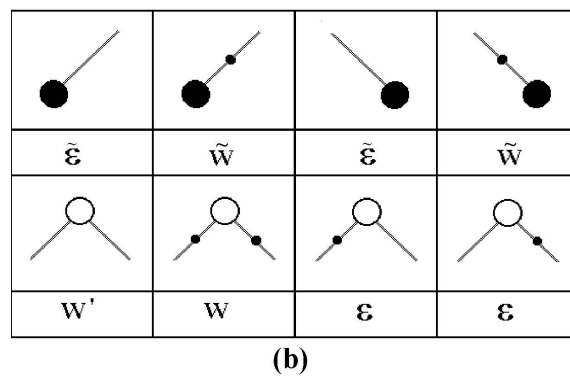
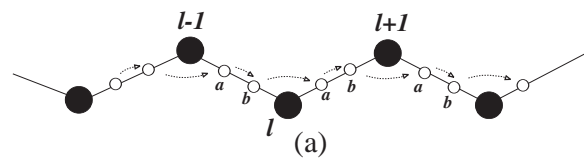


FIG. 1: N. Pavlenko et al., J. Chem. Phys.

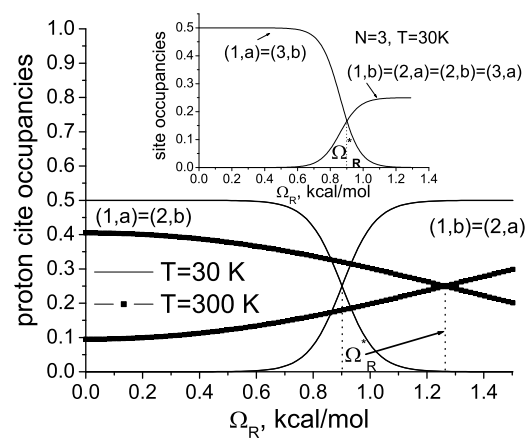


FIG. 2: N. Pavlenko et al., J. Chem. Phys.



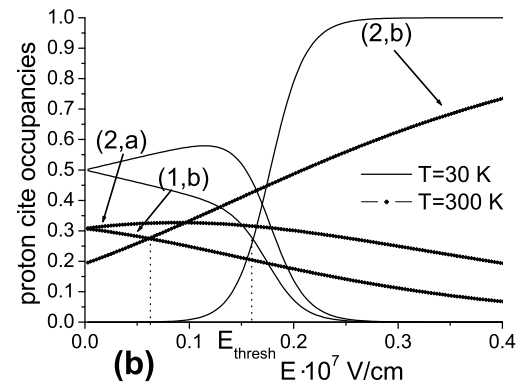
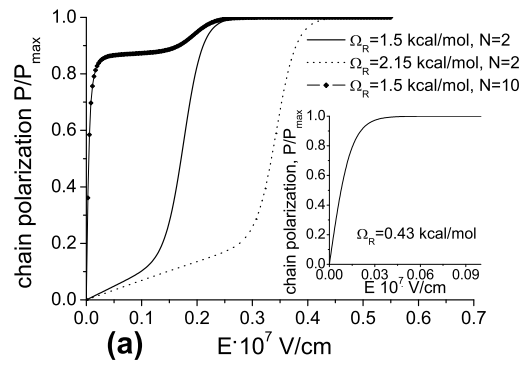


FIG. 3: N. Pavlenko et al., J. Chem. Phys.

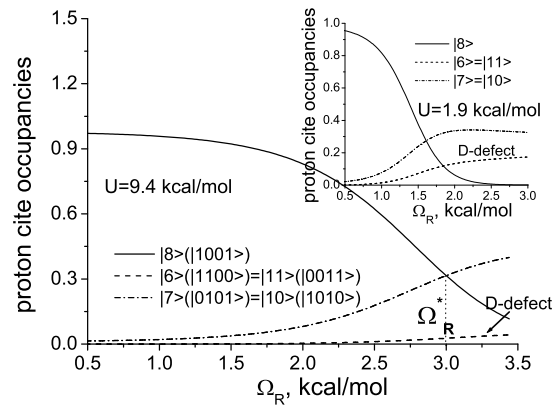


FIG. 4: N. Pavlenko et al., J. Chem. Phys.

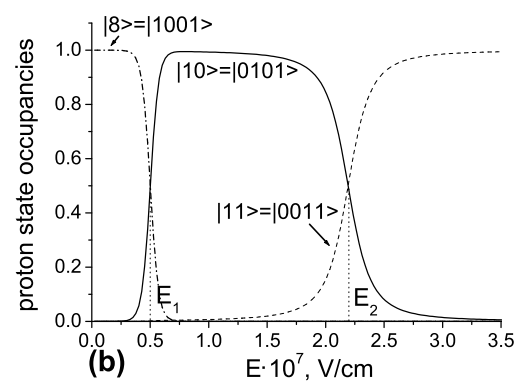
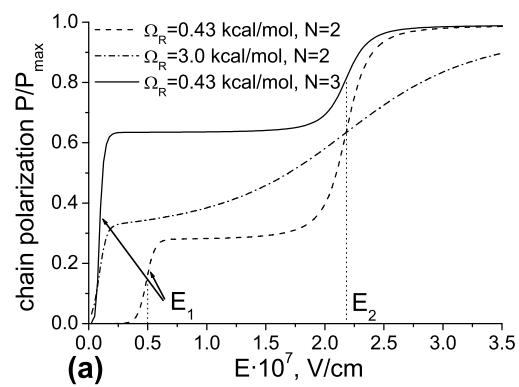


FIG. 5: N. Pavlenko et al., J. Chem. Phys.

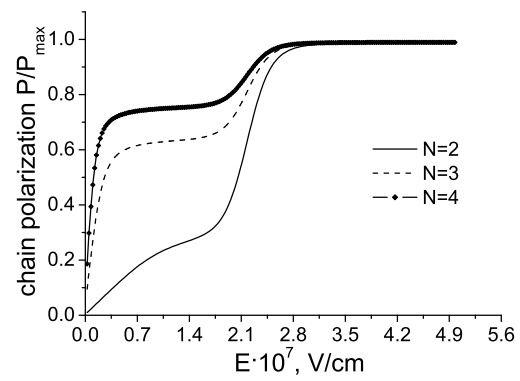


FIG . 6: N . Pavlenko et al., J. Chem . Phys.